

Identification by Proteomic Analysis of Early Post-mortem Markers Involved in the Variability in Fat Loss during Cooking of Mule Duck “Foie Gras”

Laetitia Theron,^{†,‡,#} Xavier Fernandez,^{†,‡,#} Nathalie Marty-Gasset,^{†,‡,#} Carole Pichereaux,^{Δ,§} Michel Rossignol,^{Δ,§} Christophe Chambon,[‡] Didier Viala,[‡] Thierry Astruc,[⊗] and Caroline Molette^{*,†,‡,#}

[†]INRA, UMR 1289 Tissus Animaux Nutrition Digestion Ecosystème Métabolisme, F-31326 Castanet-Tolosan, France

[‡]Université de Toulouse, INPT, UMR 1289 Tissus Animaux Nutrition Digestion Ecosystème Métabolisme, ENSAT, F-31326 Castanet-Tolosan, France

[#]ENVT, UMR 1289 Tissus Animaux Nutrition Digestion Ecosystème Métabolisme, F-31076 Toulouse, France

^ΔPlateforme Protéomique de la Génopole Toulouse Midi-Pyrénées, IPBS-FR3450, 205 route de Narbonne, 31077 Toulouse, France

[§]IPBS, Université de Toulouse, Université Paul Sabatier, F-31077 Toulouse, France,

[‡]PFEM, Composante Protéomique, INRA de Theix, F-63122 Saint Genès Champanelle, France

[⊗]INRA, UR 370 QuaPA, F-63122 Saint Genès Champanelle, France

ABSTRACT: Fat loss during cooking of duck “foie gras” is the main quality issue for both processors and consumers. Despite the efforts of the processing industry to control fat loss, the variability of fatty liver cooking yield remains high and uncontrolled. To better understand the biological basis of this phenomenon, a proteomic study was conducted. To analyze the protein fraction soluble at low ionic strength (LIS), we used bidimensional electrophoresis and mass spectrometry for the identification of spots of interest. To analyze the protein fraction not soluble at low ionic strength (NS), we used the shotgun strategy. The analysis of data acquired from both protein fractions suggested that at the time of slaughter, livers with low fat loss during cooking were still in anabolic processes with regard to energy metabolism and protein synthesis, whereas livers with high fat loss during cooking developed cell protection mechanisms. The variability in the technological yield observed in processing plants could be explained by a different physiological stage of liver steatosis.

KEYWORDS: proteomic, bidimensional electrophoresis, mass spectrometry, shotgun, fatty liver, duck, “foie gras” quality, technological yield

INTRODUCTION

France is the main producer (73%) of “foie gras” (fatty liver) of ducks or geese in the world. French foie gras is a traditional product, a coveted dish with a strong added value. The technological yield is the principal quality trait, and it is evaluated by the loss of fat during cooking. This fat loss constitutes a recurring problem for the industry and consumers because it influences the uniformity of the finished product, in terms of appearance defects (visible fat) and sensory qualities, and the profitability of a sale unit. A maximum value of 30% of fat loss during cooking is imposed by market regulation.¹ There is strong interindividual variability in the processing ability of fatty liver. Under experimental conditions, the coefficient of variation of fat loss is usually around 50%. Under industrial production, a standard practice to reduce the variability of fat loss consists of processing only a part of the livers, chosen on the basis of fresh weight. There is indeed a clear relationship between liver weight and technological yield:² the greater the liver weight, the less the technological yield. Despite this, variability in the technological quality is still high.

Until today, the research conducted on the technological yield of foie gras was mainly focused on the influence of production factors^{3,4} and technological treatments.^{2,5} Studies on the

biochemical determinism of fatty liver quality focused on lipids storage^{6,7} and membrane lipids.⁸ They failed to link the biochemistry of lipids in raw tissue with the fat loss during cooking of duck foie gras. To our knowledge, the potential role of the protein fraction has never been investigated. We therefore propose to study the expression of proteins early post-mortem to better understand the mechanisms underlying the variability in fat loss during cooking. To have an overview of the implication of proteins in the phenomenon of fat loss, we chose to study separately two protein fractions differing in their solubility and to adapt the separation method for each of these fractions. The soluble fraction at low ionic strength (LIS) was analyzed by two-dimensional electrophoresis, and the spots of interest were identified by mass spectrometry, both MALDI-TOF and LC-MS/MS. The nonsoluble fraction at low ionic strength (NS) was analyzed by a shotgun approach combining a separation by SDS-PAGE and identification of all proteins by mass spectrometry

Received: July 18, 2011

Revised: October 7, 2011

Accepted: October 17, 2011

Published: October 17, 2011

with a LC-MS/MS system. The relative quantity of proteins in relation with the technological yield for both fractions was evaluated to highlight differences explaining the phenomenon of fat loss during cooking.

MATERIAL AND METHODS

Animals, Breeding, Overfeeding, and Slaughter. Proteomic analysis was performed on a first set of animals, and validation by Western blot was performed on a second set of animals. All of the animals were bred, overfed, and slaughtered according to the following procedure. Male mule ducks (*Cairina moschata* × *Anas platyrhynchos*) were reared with access to free range until the age of 13 weeks in a poultry house under natural conditions of light and temperature at the Agricultural College of Périgueux (EPLEFPA, 24, France) following standard practices.⁸ Animals were then overfed in individual cages during 12 days, by the distribution of a soaked-corn mixture (42% grain–58% flour) twice a day. Ducks were slaughtered in the experimental slaughterhouse of the Agricultural College of Périgueux, 10 h after the last meal. The poultry house and the abattoir were located in the same place. Birds were crated in transport modules of four ducks each and transported (5 min) to the slaughter point, by groups of 20 (five crates). The first bird was slaughtered immediately after arrival and the 20th about 40 min later (slaughter rate was one bird every 2 min). Birds were electrically stunned head-only using scissor tongs and bled by ventral cutting of neck vessels. After a 5 min bleeding, the carcasses were scalded and plucked.

The experiments described here fully comply with legislation on research involving animal subjects according to the European Communities Council Directive of November 24, 1986 (86/609/EEC). Investigators were certified by the French governmental authority for carrying out these experiments (agreement 31-11.43.501).

Fatty Liver Processing. At the end of the slaughter process, 20 min after bleeding, livers were removed from the carcass and weighed. Livers were chilled on ice during 6 h and trimmed of their main blood vessels. Each fatty liver was then transversally divided in three parts including the two lobes. In the middle part of each lobe, a slice of approximately 200 g was excised and put into a glass jar. Salt (12 g/kg) and pepper (2 g/kg) were added, and the jars were cooked for 1 h in water in an autoclave (“Brouillon Process”, Sainte Bazeille, France) at 85 °C under a pressure of 0.8 bar. Temperature was controlled in the water and in two control jars equipped with temperature sensors. After 30 min of chilling (circulating cool water), the jars were stored at 4 °C for 2 months until the opening for the estimation of the technological yield.

Technological Yield Estimation. The jars were opened, and the superficial fat exuded during cooking was carefully removed from the liver. The technological yield was evaluated by the expression of fat loss during cooking as a percentage of initial liver weight:

$$\text{technological yield} = \left(\frac{\text{cooked liver weight trimmed of all visible fat}}{\text{raw liver weight}} \right) \times 100$$

Biochemical Analysis. All of these biochemical analyses were performed in duplicate on fatty livers sampled at 6 h post-mortem, after chilling.

Lipid and Nitrogen Contents. Total lipids were extracted from the raw fatty livers by homogenization in chloroform–methanol 2:1 (v/v) and measured gravimetrically according to the method of Folch et al.⁹ Total nitrogen content of fatty livers was determined using a LECO analyzer (FP 428 model) after total combustion (protein content estimation = $N \times 6.25$).

Glycogen and Lactic Acid Contents. These were measured after fatty liver homogenization in 0.5 M perchloric acid. After centrifugation

during 20 min at 2500g, the supernatant was used for both glycogen and lactic acid determination¹⁰ by enzymatic method after glycogen hydrolysis by amyloglucosidase.

Determination of Protein and Lipid Oxidation. Protein oxidation was estimated by the detection of carbonyl groups according to the method of Oliver et al.¹¹ with slight modifications for measurement in meat samples.¹² Carbonyl groups were detected by reactivity with 2,4-dinitrophenylhydrazine (DNPH) to form protein hydrazones. The results were expressed as nanomoles of DNPH fixed per milligram of protein. Lipid oxidation was measured by the thiobarbituric acid reactive substances (TBARS) according to the method of Lynch and Frey.¹³ Samples were incubated with 1% (w/v) 2-thiobarbituric acid in 50 mM NaOH and 2.8% (w/v) trichloroacetic acid in a boiling water bath for 40 min. After cooling in ice, the pink chromogen was extracted with *n*-butanol and its absorbance measured at 535 nm. TBARS concentrations were calculated using 1,1,3,3-tetramethoxypropane as standard. Results were expressed as nanomoles of malonaldehyde (MDA) per milligram of fatty liver.

Protein Extraction. The method was adapted from Sayd et al.¹⁴ and was performed on nine fatty livers selected in the group showing low technological yield (<74%) and nine others in the group showing high technological yield (>83%). Ten grams of fatty liver sampled at 20 min post-mortem was frozen in liquid nitrogen and stored at –80 °C. The samples were ground in liquid nitrogen to obtain a fine powder. They were then homogenized using a glass bead agitator MM2 (Retsch, Haan, Germany) in a low ionic strength buffer (LIS), 40 mM Tris-HCl (pH 7.4), at 4 °C in a ratio of 1:4 (w/v). The homogenate was centrifuged at 4 °C for 10 min at 10000g. The fat cake was removed, and the homogenization was done a second time. After centrifugation, the supernatant, forming the protein fraction soluble in LIS buffer, was stored at –80 °C. The pellet was washed three times with this buffer to obtain only insoluble proteins in LIS buffer. After the last centrifugation, the supernatant was removed and the pellet was homogenized in the following buffer: 7 M urea, 2 M thiourea, 4% CHAPS (w/v), at 4 °C in the same ratio as the first step. The homogenate was centrifuged at 4 °C for 10 min at 10000g. The supernatant, forming the protein fraction not soluble at low ionic strength, was stored at –80 °C. The protein concentration of both fractions was determined by using Bradford assay (Bio-Rad).

Analysis of the Protein Fraction Soluble in a Low Ionic Strength Buffer. *Bidimensional Electrophoresis.* First, 300 μg of proteins of the fraction soluble at low ionic strength was incorporated in a buffer containing 7 M urea, 2 M thiourea, 2% CHAPS (w/v), 0.4% carrier ampholyte (v/v), 1% DTT (w/v), and bromophenol blue. Samples were loaded onto immobilized pH gradients strips (pH 5–8, 17 cm, Bio-Rad), and isoelectric focusing was performed using a Protean IEF cell system (Bio-Rad). Gels were passively rehydrated for 16 h. Rapid voltage ramping was subsequently applied to reach a total of 86 kVh. The equilibration buffer contained 6 M urea, 30% glycerol, 2% SDS, and 50 mM Tris-Cl, pH 8.8. Strips were first incubated in an equilibration buffer containing 1% DTT. Strips were then incubated in a second equilibration buffer containing 2.5% iodoacetamide and bromophenol blue. After strip equilibration, proteins were resolved on 12% sodium dodecyl sulfate–polyacrylamide gel electrophoresis (SDS-PAGE) using a Protean II XL system (Bio-Rad) for the second dimension. Gels were stained with Coomassie Blue (colloidal blue) as previously described by Morzel et al.¹⁵

Image Analysis. All of the gels were analyzed with the software Image Master 2D Platinum (GE Healthcare, Uppsala, Sweden) to point out spots of interest. Per gel, each detected and matched spot was normalized by expressing its relative intensity to the total intensity of all valid spots. Spots of interest were determined by using the procedure of Meunier et al.,¹⁶ which uses fold change ratio.

Identification of the Spots of Interest of the Soluble Fraction LIS by Mass Spectrometry. Coomassie stained spots of

interest were manually excised using pipet tips. The spots were then destained with 100 μL of 25 mM NH_4HCO_3 with acetonitrile 95:5 (v/v) for 30 min, followed by two washes in 100 μL of 25 mM NH_4HCO_3 with acetonitrile 50:50 (v/v) and then dehydrated in 100% acetonitrile. Gel spots were completely dried using a Speed Vac before trypsin digestion at 37 °C over 5 h with 15 μL of trypsin (10 ng/ μL ; V5111, Promega) in 25 mM NH_4HCO_3 . Peptide extraction was optimized by adding 8 μL of acetonitrile, followed by 10 min of sonication. For matrix-assisted laser desorption/ionization–time-of-flight (MALDI-TOF) mass spectrometry analysis, 1 μL of supernatant was loaded directly onto the MALDI target. The matrix solution (5 mg/mL of α -cyano-4-hydroxycinnamic acid in 50% acetonitrile, 0.1% trifluoroacetic acid) was immediately added and allowed to dry at room temperature. Peptide Mass Fingerprint (PMF) of trypsin-digested spots was determined in positive-ion reflector mode using a Voyager DE Pro MALDI-TOF-MS (Applied Biosystems, Courtaboeuf, France). External calibration was performed with a standard peptide solution (Peptide Mix 4, Proteomix, LaserBio Laboratories, Sophia-Antipolis, France). PMFs were compared to SwissProt (01/2008, 290 484 seq) protein sequence databases [ftp://ftp.ebi.ac.uk/pub/databases/uniprot/knownledgebase/uniprot_sprot.fasta.gz] using MASCOT 2.2 software [http://www.matrixscience.com]. The initial search parameters allowed a single trypsin missed cleavage, partial carbamidomethylation of cysteine, partial oxidation of methionine, and mass deviation ≤ 25 ppm. The validations are based on the significant score ($p < 0.05$) given by Mascot software, which takes into account the number of matched peptides per protein (at least five peptides) and the decoy score. When identification by MALDI-TOF was unsuccessful, identification was also attempted using nano LC-ion trap MS/MS analysis. Six microliters of peptide mixture was analyzed by online nanoflow liquid chromatography (Ultimate LC (Dionex, Voisins le Bretonneux)). The gradient consisted of 10–90% acetonitrile in 0.5% formic acid at a flow rate of 200 nL/min for 45 min. The eluate was electrosprayed into an LCQDeca through a nanoelectrospray ion source (ThermoFisher Scientific, Les Ulis, France). Peptide ions were analyzed by the data-dependent “triple play” method: (i) full MS scan (m/z 400–1400), (ii) zoom scan (scan of the major ion with bigger resolution), and (iii) MS/MS of this ion. Identification of peptides was performed with Mascot 2.2, restricting the taxonomy to vertebrates (04/2008, 1177111 sequences) in the protein NCBI database. Mass deviation tolerance was set at 1.5 Da for parent ion and at 0.8 for fragment ions. Protein identification was validated when at least two peptides originating from one protein showed significant identification Mascot scores ($p < 0.05$). Identifications with only two unique peptides were manually validated with criteria of match fragments ions (occurrence of uninterrupted y- or b-ion series of at least three consecutive amino acids, preferred cleavages N-terminal to proline bonds, and mass accuracy).

Analysis of the Protein Fraction Not Soluble in a Low Ionic Strength Buffer.

Protein Separation. Protein preparations from the low fat loss group ($n = 9$) and the high fat loss group ($n = 9$) were reduced with 20 mM DTT and then alkylated in 60 mM chloroacetamide. Samples containing 2% (w/v) SDS, 5% β -mercaptoethanol, 10% glycerol, and 62 mM Tris-HCl, pH 6.8, in a ratio 1:1 v/v¹⁷ were heated at 95 °C for 5 min. SDS-PAGE (12% acrylamide) was performed following the method described by Laemmli¹⁷ using a Mini-Protean II electrophoresis unit. Samples were loaded at 50 μg protein per lane. Gels were run at 35 mA/gel (for Mini-Protean II), constant current, until the dye front reached the bottom of the gel. Gels were stained overnight in Coomassie Brilliant Blue G-250 (PageBlue Protein Staining Solution, FERMENTAS).

Protein Digestion. Each lane (one for each fat loss group) was systematically cut into 10 bands of similar volume for MS/MS protein identification. Each band was incubated in 25 mM ammonium bicarbonate and 50% ACN until destaining. Gel pieces were dried in a vacuum

SpeedVac (45 °C), further rehydrated with 30 μL of a trypsin solution (10 ng/L in 50 mM NH_4HCO_3), and finally incubated overnight at 37 °C. The resulting peptides were extracted from the gel as described previously.¹⁸ The trypsin digests were dried in a vacuum SpeedVac and stored at -20 °C before LC-MS/MS analysis.

Nano-LC-MS/MS Analysis. The trypsin digests were separated and analyzed by nano-LC-MS/MS using an Ultimate 3000 system (Dionex, Amsterdam, The Netherlands) coupled to an LTQ-Orbitrap mass spectrometer (Thermo Fisher Scientific, Bremen, Germany). The peptide mixture was loaded on a C18 precolumn (300 μm inner diameter, 15 cm PepMap C18, Dionex) equilibrated in 95% solvent A (5% acetonitrile and 0.2% formic acid) and 5% solvent B (80% acetonitrile and 0.2% formic acid). Peptides were eluted using a 5–50% gradient of solvent B during 80 min at 300 nL/min flow rate. The LTQ-Orbitrap was operated in data-dependent acquisition mode with the Xcalibur software (version 2.0.6, Thermo Fisher Scientific). Survey scan MS spectra were acquired in the Orbitrap over the m/z 300–2000 range with the resolution set to a value of 60000. The five most intense ions per survey scan were selected for collision-induced dissociation (CID) fragmentation, and the resulting fragments were analyzed in the linear trap (LTQ). Dynamic exclusion was used within 60 s to prevent repetitive selection of the same peptide. To automatically extract peak lists from Xcalibur raw files, the ExtractMSN macro provided with Xcalibur was used through the Mascot Daemon interface (version 2.3.2, Matrix Science, London, U.K.). The following parameters were set for creation of the peak lists: parent ions in the mass range 400–4500, no grouping of MS/MS scans, and threshold at 1000. A peak list was created for each fraction analyzed (i.e., gel slice), and individual Mascot searches were performed for each fraction.

Database Search. MS/MS spectra were processed by Mascot software against the *Gallus gallus* (SwissProt-TrEmbl) and *Cairina moschata*–*Anas platyrhynchos* (NCBI) databases. The following search parameters were applied: trypsin as cleaving enzyme, “ESI-Trap” as instrument, peptide mass tolerance of 10 ppm, MS/MS tolerance of 0.8 Da, and one missed cleavage allowed. Methionine oxidation was chosen as variable modification.

Bioinformatic Analysis. Validation and Semiquantitation. The MFPAQ software¹⁹ was used to validate the results (1.3% FDR) and to analyze the data. This software is a Web application that allows fast and user-friendly verification of Mascot result files as well as data quantification. In particular, the spectral counts corresponding to each identified protein were extracted from each analysis.^{20,21} Taking into account the molecular weight of proteins, we define an abundance index (PAI): PAI = spectral counts/molecular weight \times 2500. This index allows us to classify in a semiquantitative way the proteins inside each sample.

Functional Analysis. The proteins validated by the software MFPAQ were introduced in the Protein Center software (Proxeon, Odense, Denmark; http://www.proteincenter.proxeon.com), where they were clustered with a criterion of 60% homology. Analysis of the functional distribution of groups is then done, taking into account the classification established by “Genome Ontology”.

Western Blot of Mitochondrial Carrier Protein Homologue (MIMP). The NS fraction was used to perform Western blots of MIMP using samples from the second experiments (independent samples). Following SDS-PAGE, gel was steeped in transfer buffer containing 25 mM Tris, 192 mM glycine, and 20% v/v methanol²² during 10 min. The proteins were transferred to nitrocellulose membrane (Hybond ECL, Amersham) at 100 V during 30 min using a transfer cell (Criterion Blotter, Bio-Rad). Membrane was blocked with milk buffer containing 3% w/v milk powder in phosphate buffer saline (PBS, pH 7.5) at room temperature for 1 h. Following blocking, membrane was probed for specific proteins using primary antibody (goat anti-MIMP, sc-79980 Santa Cruz Biotechnology, Inc.) overnight at 4 °C. The primary antibody to milk buffer ratio was 1:500. Then, the membrane was washed

Table 1. Technological Yield and Biochemical Characteristics of the Fatty Livers^a

	low fat loss	high fat loss	significance
fatty liver weight, g	570 ± 44	566 ± 42	NS
technological yield, %	88.8 ± 4.3	68.2 ± 6.1	$p < 0.001$
lipid content, %	57.6 ± 2.0	58.6 ± 1.8	NS
protein content, %	7.6 ± 0.8	7.0 ± 0.5	NS

^a For each fat loss group ($n = 9$), results are reported as the mean value ± standard deviation. NS, nonsignificant.

three times with PBS buffer and incubated in secondary antibody (rabbit anti-goat IgG-HRPsc-2768, Santa Cruz Biotechnology, Inc.) at room temperature for 1 h. The secondary antibody to milk buffer ratio was 1:10000. Following this incubation, the membrane was washed three times with PBS buffer, and the chemiluminescent substrate (Super Signal West Pico, Thermo-Pierce) was then used to detect the reactivity of the primary antibody with its antigen. Photographs of the Western blot were taken by making a contact between the membrane and a photo film (Amersham HyperfilmMP, GE Healthcare). The film was then developed by steeping in 20% revelation solution (AL4, Kodak), distilled water, and 20% fixation solution (LX24, Kodak) for 1 min each, respectively. The pool of samples was used as a reference. Band intensity of samples was then measured by using Image Analysis (ImageMaster 2D Platinum 6.0, GE Healthcare). It was expressed as a percentage of reference protein.

Statistical Analysis. To determine the significance of fat loss during cooking, a t test was used to analyze biochemical data and MIMP protein band intensities. Results are expressed as the mean ± standard deviation.

RESULTS AND DISCUSSION

The aim of this proteomic study was to identify differential protein expression early post-mortem according to fat loss during cooking of duck fatty livers. The liver weight, as well as the lipid and protein contents, is known to affect the technological yield.² That is why the comparison was conducted on two groups showing significant differences only for the yield ($p < 0.001$) but similar liver weight and lipid and protein contents (Table 1).

Low Ionic Strength Protein Fraction. The image analysis performed on 2D gels allowed the matching of 187 spots. By comparing the proteomic maps at 20 min post-mortem of high and low fat loss groups, the statistical analysis revealed 47 spots of interest (Figure 1). Early post-mortem, 8 and 4 spots were overexpressed in the high and low fat loss groups, respectively; 1 was detected only in the high fat loss group, and 34 were detected only in the low fat loss group. The use of both MALDI-TOF-MS and LC-MS/MS allowed the identification of 13 proteins (Table 2). The sequences were identified by comparison with *G. gallus* and *A. platyrhynchos* databases. The 13 proteins identified could be classified according to their biological functions: four were involved in metabolism, four in cellular oxidative stress, and one in calcium homeostasis; one had a proteolytic activity, one took part in ATP synthesis, and two were miscellaneous proteins.

Metabolism. Among the 13 proteins identified in the LIS protein fraction, 4 are involved in energy metabolism. Triosephosphate isomerase 1 (spot 302), α -enolase (spot 100), and malate dehydrogenase (spot 138) were detected only in the low fat loss group, whereas fatty acid binding protein 4 (FABP4) (spot 304) was detected only in the high fat loss group. Triosephosphate isomerase 1 and α -enolase are glycolytic enzymes, responsible

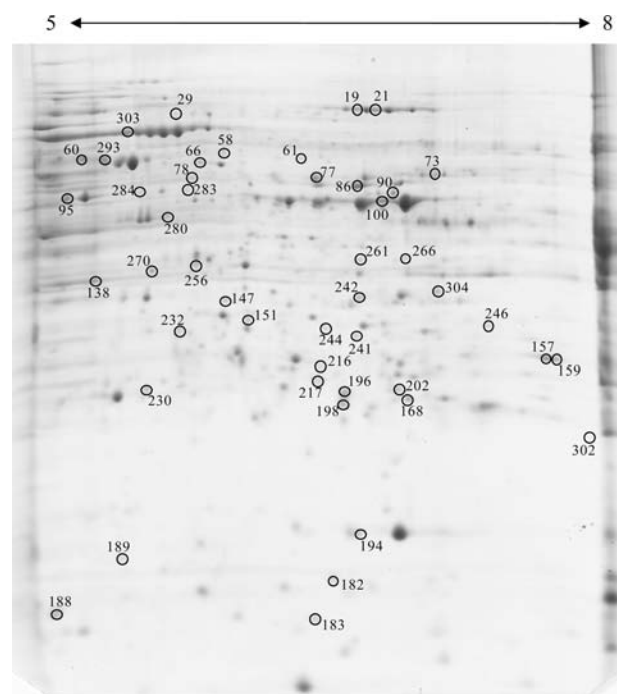


Figure 1. Representative two-dimensional gel electrophoresis map of duck fatty liver. The first dimension was performed between pH 5 and 8. The second-dimension gel contains 12% acrylamide. Three hundred micrograms of proteins was loaded. The black circles indicate the differentially expressed proteins.

for the fifth and ninth steps of glycolysis, respectively. Malate dehydrogenase is an enzyme of the citric acid cycle that catalyzes the reversible conversion of malate into oxaloacetate, using NAD^+ . This enzyme is also involved in gluconeogenesis. Fatty acid binding protein 4 is involved in carbohydrate biosynthesis. We measured the glucose and lactic acid contents in both groups of fat loss during cooking. We found a higher quantity of glycogen in livers that will have a low fat loss during cooking and an equal quantity of lactic acid in both groups (Figure 2). We hypothesized that in these livers, the glycolytic metabolism was still efficient because they have enough energetic resources. At the end of the overfeeding process, lipid metabolism is enhanced in geese livers as shown by gene expression profile²³ and in duck livers as found by proteomic analysis,²⁴ whereas overfeeding has a down-regulative effect on genes involved in glycolysis in geese livers.²³ In our study, the livers were sampled at the end of the process of overfeeding. Our results revealed that in the low fat loss group, there was an overexpression of proteins involved in metabolism. These livers may still be in a dynamic process of lipid synthesis and storage. Furthermore, the expression of the *FABP4* gene is related to human liver fat content in nonalcoholic fatty liver disease.²⁵ We built experimental groups with equivalent lipid content so we cannot correlate the expression of proteins with this parameter, but because of this relationship in human disease, we can speculate that the overexpression of *FABP4* in the high fat loss group might be a marker of a protective reaction of the liver. This result leads us to draw the hypothesis that the livers which will show a high fat loss during cooking have developed before slaughter cell protection mechanisms.

Cellular Oxidative Stress. Four spots identified in the LIS protein fraction were related to oxidoreduction process: one was

Table 2. Identification of Spots from LIS Protein Fraction for Which Expression Early Post-mortem Was Linked to Fat Loss during Cooking

sequence ref ^a	spot no.	low fat loss	high fat loss	protein name; ^a taxonomy	score Mascot ^b	sequence coverage, ^c %	no. of peptides matched ^d	theor MW, ^e kDa	theor pI ^f
FTNGVNY03F0Z2Y.s.ap.2	302	1.15 ± 0.53	ND	Metabolism triosephosphate isomerase; <i>Anas platyrhynchos</i>	108	37	14	43668	8.77
M20749.s.ap.2	100	0.20 ± 0.21	ND	α enolase 1; <i>Anas platyrhynchos</i>	110	36	17	61834	8.42
FTNGVNY03F0BE0.s.ap.2	138	0.52 ± 0.55	ND	malate dehydrogenase cytoplasmic-like; <i>Anas platyrhynchos</i>	75	15	8	58602	8.85
DQ358123.s.ap.2	304	ND	0.36 ± 0.59	fatty acid binding protein 4; <i>Anas platyrhynchos</i>	120	44	15	23747	8.50
gill18093103	196 ^f	0.56 ± 0.32	0.34 ± 0.19	Oxidoreduction Process Prdx3 protein; <i>Gallus gallus</i>	155	8	2	30972	8.40
gill18093103	168 ^f	0.10 ± 0.03	0.28 ± 0.10	Prdx3 protein; <i>Gallus gallus</i>	77	8	2	30972	8.40
F3_T72ZM05F2QQ6.s.ap.0.2	194 ^f	0.12 ± 0.03	0.66 ± 0.27	superoxide dismutase 1; <i>Anas platyrhynchos</i>	68	32	6	32279	8.52
gill224071287	86 ^f	0.34 ± 0.06	1.58 ± 0.75	aldehyde dehydrogenase 2; <i>Taeniopygia guttata</i>	181	11	5	56746	6.68
FTNGVNY03GIRIX.s.ap.2	256	0.14 ± 0.20	ND	Cellular Calcium Ion Homeostasis regucalcin; <i>Anas platyrhynchos</i>	93	34	13	43725	8.18
gill259835	188 ^f	0.26 ± 0.25	ND	Proteolytic Activity preprocathepsin D; <i>Gallus gallus</i>	112	8	2	43270	5.90
FTNGVN Y03F3RUW.s.ap.0.2	95	0.31 ± 0.18	ND	ATP Synthesis ATP synthase subunit β ; <i>Anas platyrhynchos</i>	143	47	21	54441	5.11
gill7658009	182	0.32 ± 0.34	0.21 ± 0.12	Miscellaneous protein kinase C inhibitor; <i>Anas platyrhynchos</i>	70	60	6	13697	6.04
GIDS3QQ2DOEUG.s.ap.2	242	0.12 ± 0.04	0.44 ± 0.39	agmatinase; <i>Anas platyrhynchos</i>	77	20	9	42733	8.65

^a Protein name and sequence reference were derived from Swiss-Prot database and EST database. ^b The MASCOT baseline significant score is 67. ^c Percent of coverage of the entire amino acid sequence. ^d Number of matched peptides in the database search. ^e Molecular weight (MW) and pI theoretical (recorded in UniProtKB/Swiss-Prot databases for MALDI-TOF and NCBI database vertebrates taxonomy for LC-MS/MS). ^f Preprocathepsin D (spot 188), Prdx3 protein (spots 168 and 196), superoxide dismutase 1 (spot 194), and aldehyde dehydrogenase 2 (spot 86) were identified by LC-MS/MS.

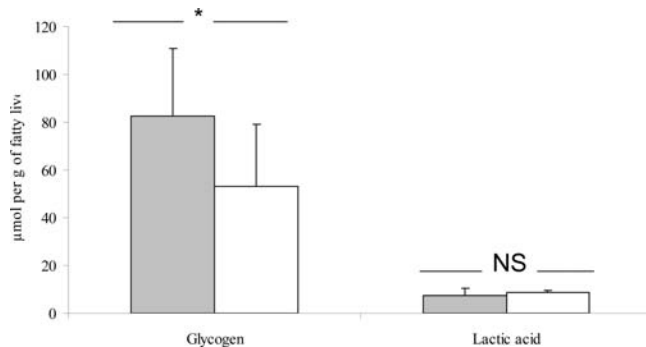


Figure 2. Glycogen and lactic acid measurements in duck fatty livers showing low (gray) and high (white) fat loss during cooking. For each fat loss group ($n = 9$), results are reported as the mean value \pm standard deviation and are expressed as micromoles per gram of raw fatty liver. NS, nonsignificant; *, $p < 0.05$.

overexpressed in the low fat loss group, that is, the peroxiredoxin protein III (Prdx3; spot 196), and three were overexpressed in the high fat loss group, that is, Prdx3 protein (spot 168), superoxide dismutase 1 (SOD-1; spot 194), and aldehyde dehydrogenase 2 (spot 86). SOD-1 is a peroxisomal free radical scavenging enzyme that dismutates reactive oxygen species to hydrogen peroxide and molecular oxygen. Removal of superoxide radicals by SOD prevents formation of very active hydroxyl radicals. Prdx3 and aldehyde dehydrogenase 2 are involved in redox regulation of the cell. To validate the physiological significance of the identified proteins, we determined the oxidation states of proteins and lipids. For this purpose, we compared the amount of carbonyl groups and TBARS between low and high fat loss group. The results did not show significant differences (Figure 3). We assume that the lack of specificity and sensitivity of the method²⁶ and the individual variability found in the biochemical analysis do not allow us to link oxidative stress to fat loss mechanisms. In a proteomic analysis of mice livers by iTRAQ, Iff et al.²⁷ showed that SOD-1 was up-regulated in the livers of STAT6 (signal transducer and activator of transcription) knockout mice. In STAT6-null mice, liver lipid content was significantly increased when compared to the wild type controls. Cu/Zn SOD gene expression was diminished in subjects with cirrhosis secondary to NASH when compared with healthy controls.²⁸ During overfeeding of mule ducks, the expression of antioxidant proteins is increased.²⁴ From this, the expression of SOD at the level of the gene or the protein is still contradictory. Nevertheless, because reactive oxygen species accumulation leads to oxidative stress, the latter being enhanced with lipid accumulation, the livers may have developed a protective system due to the steatosis stage. Both fat loss groups present antioxidant proteins, but in the case of livers that will have a high fat loss during cooking, they might have more intense oxidative stress because of a more advanced stage of steatosis. We calculated the correlations between the technological yield and spots intensities. The Prdx3 protein (spot 168) intensity showed a correlation of -0.67 ($p = 0.03$), the SOD-1 (spot 194) intensity showed a correlation of -0.62 ($p = 0.07$), and the aldehyde dehydrogenase 2 (spot 86) intensity showed a correlation of -0.59 ($p = 0.07$). The intensities of the three spots overexpressed in the high fat loss group are negatively correlated with the technological yield, emphasizing our hypothesis of increased oxidative stress in high fat loss livers. These results indicate that the more these proteins

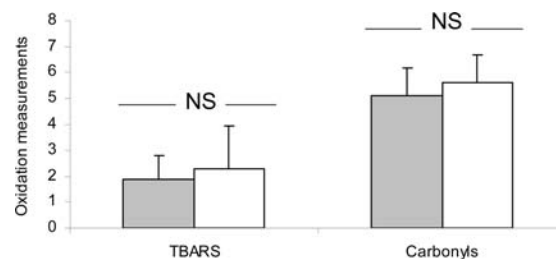


Figure 3. Lipid and protein oxidation evaluation by detection of TBARS species and carbonyl groups, respectively, in duck fatty livers showing low (gray) and high (white) fat loss during cooking. TBARS species are expressed as nanomoles of malonaldehyde per milligram of fatty liver, and carbonyl groups are expressed as nanomoles of DNPH per milligram of proteins. For each fat loss group ($n = 9$), results are reported as the mean value \pm standard deviation. NS, nonsignificant.

were expressed, the less the technological yield was and so the higher the fat loss during cooking of fatty livers.

Calcium Homeostasis. In the LIS protein fraction, one protein was found to be a part of cellular calcium homeostasis: regucalcin (spot 256), which is detected only in low fat loss group. Regucalcin is a calcium-binding protein that plays a multifunctional role in liver cells.²⁹ Because regucalcin can be involved in many processes in liver cells, it is difficult to comment on its up-regulation in the low fat loss group. Nevertheless, the expression of hepatic regucalcin mRNA is enhanced in regenerating rat liver after hepatectomy.³⁰ Furthermore, in a proteomic analysis of mice livers by iTRAQ, Iff et al.²⁷ showed that regucalcin was up-regulated in the livers of STAT6 knockout mice. The livers that will have a low fat loss during cooking may be still in development and in adaptation process to lipid synthesis due to the high amount of dietary glucose intake. This is consistent with the increase of regucalcin expression at the end of the overfeeding in mule ducks, already reported in the proteomic study.²⁴

Proteolytic Activity. Preprocathepsin D (spot 188) is detected only in low fat loss group. Preprocathepsin D is the inactive form of cathepsin D, which is a lysosomal aspartic protease. Cathepsin D is a major lysosomal enzyme involved in protein degradation. To our knowledge, few studies are available on the role of cathepsin D in steatosis. Cathepsin D appears to act as part of the effector protease cascade in hepatocyte apoptosis.³¹ The expression of preprocathepsin D in the low fat loss group does not mean necessarily a more intense proteolysis or an enhanced apoptotic pathway. Further studies are needed to conclude on this point.

ATP Synthesis. Spot 95 was identified as the ATP synthase subunit β , detected only in the low fat loss group. The expression of this protein in only the low fat loss group may reflect a higher energy production in the livers constituting this group. This protein could be a good marker of the phenomenon studied here because this spot was not detected in the proteomic analysis of livers with a low technological yield.

Miscellaneous. The protein kinase C inhibitor (spot 182) was overexpressed in the low fat loss group. Because of the large spectrum of activities of this protein, we cannot reach a clear hypothesis on its contribution to the variability in liver quality. The agmatinase (spot 242) was overexpressed in the high fat loss group. Agmatinase hydrolyzes agmatine to putrescine and urea. Agmatinase was found to be up-regulated in a proteomic analysis of mouse livers with nonalcoholic fatty liver induced by a high-fat

Table 3. Identification of Proteins Detected Only in the Low Fat Loss Group in the NS Protein Fraction^a

sequence ref	protein name; taxonomy	CC	BP	MF	sequence coverage	peptide count	PAI
Q98TH5	ribosomal protein S11; <i>Gallus gallus</i>	Ri	MP	Str	28.5	5	44.3
Q5ZK18	putative uncharacterized protein; <i>Gallus gallus</i>	Cy	MP	CA	10.3	3	42.7
Q6ITC7	40S ribosomal protein S13; <i>Gallus gallus</i>	Ri	MP	Str	33.1	3	39.7
Q5F412	putative uncharacterized protein; <i>Gallus gallus</i>	Csk	CO	PB	25.8	2	33.7
Q6EE61	ribosomal protein L17 (fragment); <i>Gallus gallus</i>	Ri	MP	Str	27.4	4	31.8
Q5ZJ12	putative uncharacterized protein; <i>Gallus gallus</i>	Cy			18.7	6	31.7
P08636	40S ribosomal protein S17; <i>Gallus gallus</i>	Ri	MP	Str	45.9	3	29.6
Q08200	60S ribosomal protein L10 (fragment); <i>Gallus gallus</i>	Ri	MP	Str	22.4	5	28.6
Q9PVL6	mitochondrial carrier homologue 2; <i>Gallus gallus</i>	Mb	T		23.1	4	23.4
Q5ZLE6	eukaryotic translation initiation factor 3 subunit H; <i>Gallus gallus</i>	Cy	CO	TA	19.8	3	23.0
Q3YI09	5'-AMP-activated protein kinase γ -1 noncatalytic subunit variant 2; <i>Gallus gallus</i>		MP	CA	23.2	6	21.7
Q5ZLA5	eukaryotic translation initiation factor 3 subunit E; <i>Gallus gallus</i>	Cy	CO	TA	13.3	5	20.2
Q5ZK70	putative uncharacterized protein; <i>Gallus gallus</i>		MP	CA	6.5	2	16.2
Q5F3N1	protein-;isoaspartate (D-aspartate) O-methyltransferase; <i>Gallus gallus</i>	Cy	MP	CA	22.4	3	13.2
Q5ZIV0	serine/threonine-protein phosphatase; <i>Gallus gallus</i>	Cy	MP	CA	9.8	3	13.1
Q5ZLL5	ubiquinone biosynthesis methyltransferase C0Q5, mitochondrial; <i>Gallus gallus</i>	Cy	MP	CA	15.8	3	12.9
013268	proteasome subunit α type-7; <i>Gallus gallus</i>	Pr	MP	CA	13.7	2	12.0
Q9I8D4	fructose-1,6-bisphosphatase (fragment); <i>Gallus gallus</i>	Cy	MP	CA	7.7	2	11.9
Q5ZJZ5	D- β -hydroxybutyrate dehydrogenase, mitochondrial; <i>Gallus gallus</i>	Mb	MP	CA	12.7	1	11.8
B3TZB3	CGI-58; <i>Gallus gallus</i>	Mb	MP	CA	14.3	4	11.7
Q5ZIP1	putative uncharacterized protein; <i>Gallus gallus</i>	Cy	MP	CA	11.6	1	11.6
Q95HB3	MHC class I antigen α chain; <i>Anas platyrhynchos</i>	Mb	RS			9	11.3
Q156C7	5'-AMP-activated protein kinase β -2 nocalytic subunit transcript variant 2; <i>Gallus gallus</i>			CA	15	2	10.9
Q5ZLQ7	putative uncharacterized protein; <i>Gallus gallus</i>	Cy	CO		12.3	4	10.7
A9CP13	D-serine dehydratase (fragment); <i>Gallus gallus</i>	Mb			13.6	3	10.6
Q5ZIV8	putative uncharacterized protein; <i>Gallus gallus</i>	Mb	CDi	PB	14.7	2	10.0
Q5ZIG4	putative uncharacterized protein; <i>Gallus gallus</i>	Cy	MP	CA	14.6	1	10.0
Q5ZJ93	putative uncharacterized protein; <i>Gallus gallus</i>	Cy	MP	CA	11.4	2	9.3
Q5ZHT1	acyl-CoA dehydrogenase family member 11; <i>Gallus gallus</i>	Cy	MP	CA	8.5	5	9.0
Q5ZKX8	putative uncharacterized protein; <i>Gallus gallus</i>	Cy	MP	TA	9.1	2	8.6
Q5ZLP8	insulin-like growth factor 2 mRNA-binding protein 3; <i>Gallus gallus</i>	Cy	RBP	TA	9.1	2	8.6
B6V3H7	CAPN1; <i>Gallus gallus</i>	Mb	MP	CA	7.9	5	8.5
Q0KKP4	lanosterol 14 α -demethylase; <i>Gallus gallus</i>	Mb	MP	CA	8.1	3	8.5
Q2LAI0	5'-AMP-activated protein kinase α -2 catalytic subunit; <i>Gallus gallus</i>	Mb	MP	CA	7.4	1	7.2
Q2PUH1	5'-AMP-activated protein kinase α -1 catalytic subunit; <i>Gallus gallus</i>	Mb	MP	CA	8.9	3	7.1
P13216	adrenodoxin, mitochondrial (fragment); <i>Gallus gallus</i>	Cy	MP	CA	6.3	1	7.0
B2M0K4	ADP-dependent glucokinase; <i>Cairina mosckata</i>	Mb	MP	CA		1	6.8
Q5ZL59	ubiquitin carrier protein; <i>Gallus gallus</i>		RBP	CA	7.5	1	6.8
Q5F353	putative uncharacterized protein; <i>Gallus gallus</i>	Go	T	PB	7.3	1	6.8
Q90997	transferrin receptor protein 1; <i>Gallus gallus</i>	Mb	CO	CA	6.1	2	6.4
P20678	cytochrome P450 2H2; <i>Gallus gallus</i>	Mb	MP	CA	4.1	1	6.1
Q8UUX5	GDP/GTP exchange factor VAV2; <i>Gallus gallus</i>	Mb	RBP	MB	5.1	3	6.0
Q5ZL25	putative uncharacterized protein; <i>Gallus gallus</i>	Cy	CO	TA	8.8	2	5.7
Q5ZHM0	putative uncharacterized protein; <i>Gallus gallus</i>		MP	CA	5.6	2	5.6
Q5ZL61	putative uncharacterized protein; <i>Gallus gallus</i>	Mb	T	NB	8	2	5.5
Q5ZK08	putative uncharacterized protein; <i>Gallus gallus</i>	Cy	MP	CA	5.9	2	5.4
	Ig Y heavy chain (7.8S); <i>Anas platyrhynchos</i>					3	5.2
Q5ZLB8	putative uncharacterized protein; <i>Gallus gallus</i>	Mb	CO	CA	5.7	1	5.2
Q5ZLD4	transmembrane protein 11; <i>Gallus gallus</i>	Mb		PB	8.2	1	5.2
Q5F4B5	putative uncharacterized protein; <i>Gallus gallus</i>	Cy	MP	CA	4.5	1	4.7
Q805C1	glycogen synthase (fragment); <i>Gallus gallus</i>		MP	CA	3.8	1	4.2
042133	μ -calpain large subunit; <i>Gallus gallus</i>		MP	CA	3.4	1	4.2

Table 3. Continued

sequence ref	protein name; taxonomy	CC	BP	MF	sequence coverage	peptide count	PAI
Q5ZMR2	putative uncharacterized protein; <i>Gallus gallus</i>	Cy	MP	CA	1.9	1	4.2
Q5F430	putative uncharacterized protein; <i>Gallus gallus</i>		MP	TA	4.3	1	4.1
Q5ZHQ6	acyl-CoA-binding domain-containing protein 5; <i>Gallus gallus</i>	Mb	T		6.3	2	4.1
Q5ZMU8	putative uncharacterized protein; <i>Gallus gallus</i>	Go	CO	PB	3.4	1	3.9
Q1HFX8	MHC class II antigen β chain; <i>Cairina mosckata</i>	Mb	RS			1	3.9
Q5ZJV9	CCR4-NOT transcription complex subunit 7; <i>Gallus gallus</i>	Nu	RBP	TA	3.5	1	3.5
042094	α 1 integrin; <i>Gallus gallus</i>	Mb	CM	Sig	3.8	2	3.4
Q5ZHL0	V-type proton ATPase subunit d 2; <i>Gallus gallus</i>	Mb	MP	CA	4.3	1	2.8
Q5ZMS0	putative uncharacterized protein; <i>Gallus gallus</i>	Nu	CO	NB	2.2	2	2.8
Q90748	brush border myosin IB; <i>Gallus gallus</i>	Csk	CO	NB	2.8	2	2.7
P18652	ribosomal protein S6 kinase 2 α ; <i>Gallus gallus</i>	Mb	MP	CA	33	2	2.7
P98157	isoform 1 of low-density lipoprotein receptor-related protein 1; <i>Gallus gallus</i>	Mb	CO	MB	1.4	2	2.6
Q5F3I9	putative uncharacterized protein; <i>Gallus gallus</i>	Cy	MP	CA	2.7	1	2.6
Q5ZK65	putative uncharacterized protein ; <i>Gallus gallus</i>	Go	T	PB	2.8	1	2.3
Q5ZIJ9	E3 ubiquitin-protein ligase MIB2; <i>Gallus gallus</i>	Cy	RBP	CA	2.2	1	2.1
Q5F3Q3	putative uncharacterized protein; <i>Gallus gallus</i>		RBP	CA	2.2	1	1.9
Q9PW08	aminopeptidase (fragment); <i>Gallus gallus</i>	Cy	MP	CA	2.1	1	1.8
OSZJT0	ATP-dependent RNA helicase SUPV3L1, mitochondrial; <i>Gallus gallus</i>	Cy	MP	CA	1.5	1	1.3

^aThe main cellular component (CC), biological process (BP), and molecular function (MF) are presented for each protein. The peptide count corresponds to peptide with a FDR < 1.3%. The protein abundance index (PAI) is calculated as indicated under Materials and Methods. Abbreviations: (cellular component) Cy, cytoplasm; Csk, cytoskeleton; EC, extracellular; Go, Golgi apparatus; Mb, membrane; Nu, nucleus; Pr, proteasome; Ri, ribosome; Sp, spliceosome; (biological process) CC, cell communication; CDi, cell differentiation; CM, cell motility; CO, cell organization; COa, coagulation; DR, defense response; MP, metabolic process; RBP, regulation of biological process; RS, response to stimulus; T, transport; (molecular function) CA, catalytic activity; E, enzyme regulator activity; MB, metal ion binding; NB, nucleotide binding; PB, protein binding; Sig, signal transducer activity; Str, structural molecule activity; T, transporter activity; TA, translation regulator activity.

diet.³² In the same study, histological observations showed that these mice developed macrovesicular steatosis without necrosis, inflammation, or fibrosis. It seems that even if our previous results showed that the livers from the high fat loss group were in a more advanced stage of steatosis, they are not in a pathological state.

Nonsoluble at Low Ionic Strength Protein Fraction. The shotgun method applied to the NS protein fraction resulted in the detection and identification of 784 proteins in both groups of fat loss during cooking. They were grouped in 615 clusters with 60% sequence homology by using the software ProteinCenter (Proxeon, Odense, Denmark; <http://www.proteincenter.proxeon.com>). The comparison of clusters of proteins showed that 70 groups were detected only in low fat loss sample (Table 3) and 71 in high fat loss sample (Table 4). An abundance index (PAI, Protein Abundance Index) was determined from the spectral counts. It was used to evaluate the relative amounts of proteins in the specific groups of the two groups. In both tables, for each protein, the main cellular component, biological process, and molecular function are presented. In both groups of fatty livers, the proteins were mainly from cytoplasm and membrane (Figure 4).

In the high fat loss group, the comparison of the proteins with the GO database did not show the predominance of a cellular component, biological process, or molecular function but two groups of proteins each containing just one protein having a strong value of PAI. We thought it interesting to study more especially these proteins because of their overexpression within the sample of high fat loss. These proteins were identified as heat shock protein 27 (HSP 27) and α isoform of calponin-1. The protein HSP 27 contributes to the stabilization of intracellular

actin filaments and could play a regulatory role in the organization of the cytoskeleton. An overexpression of HSP 27 in plasma was found in human patients with liver disease, associated with oxidative stress.³³ Calponin is an actin binding protein and is implicated in the regulation and modulation of smooth muscle contraction. A proteomic analysis of human liver revealed that calponin reflects a contribution of activated stellate cells to chronic liver injury.³⁴ Calponin is one of the markers expressed by differentiated hepatic stellate cells.³⁵ Hepatic stellate cells play a main role in excessive production and accumulation of extracellular matrix in liver fibrosis. The overexpressions of these two proteins may traduce a mechanism of defense of the tissue and a protective effect of the integrity of the cells. This can be consistent with the previous results found in the analysis of the protein fraction soluble at low ionic strength: the fatty livers that will have a high fat loss during cooking seem not to be in a synthesis process anymore but rather in protective mechanisms against lipid accumulation.

In the low fat loss group, the comparison of the groups of proteins with the GO database revealed that 13 groups of proteins over-represented were mainly from the ribosome ($p = 5.3 \times 10^{-5}$), involved in translation process ($p = 2.3 \times 10^{-3}$), and corresponded to the function of structural constituent of ribosome ($p = 5.2 \times 10^{-5}$) (Table 5). Ribosomal proteins are up-regulated during overfeeding of geese.²³ Moreover, translation factors were found to be overexpressed during overfeeding of ducks²⁴ and geese.²³ This is consistent with the increase in the protein quantity during the beginning of the period of fat accumulation in livers.^{36,37} The overexpression of ribosomal proteins at 20 min post-mortem within the group of low fat loss during cooking could be consistent with the hypothesis of

Table 4. Identification of Proteins Detected Only in the High Fat Loss Group in the NS Protein Fraction^a

sequence ref	protein name; taxonomy	CC	BP	MF	sequence coverage	peptide count	PAI
Q00649	heat shock protein 27; <i>Gallus gallus</i>	Mb	CDi	PB	37.8	6	46.6
P26932	isoform α of calponin-1; <i>Gallus gallus</i>		CO	PB	26.7	7	44.5
Q5ZMV5	actin-related protein 2/3 complex subunit 5; <i>Gallus gallus</i>	Csk	RBP	PB	37.7	4	33.1
D0VX27	mitochondrial ubiquinol-cytochrome <i>c</i> reductase 7.2 kDa protein; <i>Gallus gallus</i>	Mb	MP	CA	27.9	1	32.8
057535	nucleoside diphosphate kinase; <i>Gallus gallus</i>	Mb	CDi	CA	39.2	4	32.7
Q5ZL50	profilin; <i>Gallus gallus</i>	Csk	CO	PB	42.9	4	28.6
C7EC61	ferrochelatase; <i>Anas platyrhynchos</i>	Cy	MP	CA		4	28.2
Q5F425	protein lin-7 homologue C; <i>Gallus gallus</i>	Mb	RBP	PB	21.8	3	25.4
Q5ZLJ0	putative uncharacterized protein (fragment); <i>Gallus gallus</i>	Cy	CDi	CA	38.8	4	24.2
P84175	40S ribosomal protein S12; <i>Gallus gallus</i>	Ri	RBP	Str	13.6	2	22.7
Q25QX5	BASH/BLNK N-terminal associated protein 1; <i>Gallus gallus</i>	Mb			16.9	4	21.1
Q01841	protein-glutamine γ -glutamyltransferase 2; <i>Gallus gallus</i>		MP	CA	12	8	20.3
Q5ZLI2	proteasome subunit α type; <i>Gallus gallus</i>	Pr	MP	CA	15.7	5	19.6
Q800K9	surfeit locus protein 4; <i>Gallus gallus</i>	Mb		PB	19.7	4	18.6
Q6EE30	eukaryotic translation elongation factor 1; <i>Gallus gallus</i>	Cy	MP	TA	8	5	18.3
P50655	ATP synthase protein 8; <i>Anas platyrhynchos</i>	Mb	MP	CA		1	18.2
Q5ZLG6	putative uncharacterized protein; <i>Gallus gallus</i>		Coa	MB	8.4	2	17.3
B2M0J6	Mn superoxide dismutase; <i>Cairina moschata</i>		MP	CA		2	16.9
Q66VY4	splicing factor 3a subunit 2; <i>Gallus gallus</i>	Mb	CC	Str	17.5	3	15.9
Q9DF58	integrin-linked kinase; <i>Gallus gallus</i>	Mb	RBP	CA	10.8	3	15.5
Q05423	fatty acid-binding protein, brain; <i>Gallus gallus</i>	Cy	T	T	14.4	2	15.2
Q5ZKX9	ER lumen protein retaining receptor 2; <i>Gallus gallus</i>	Mb	CO	Sig	10.4	2	14.2
Q5F387	putative uncharacterized protein; <i>Gallus gallus</i>	Sp		MB	11	2	14.0
A7WPN2	putative uncharacterized protein LOC769360; <i>Anas platyrhynchos</i>	Mb	T			1	13.3
042479	ferrochelatase, mitochondrial; <i>Gallus gallus</i>	Mb	MP	CA	10.7	1	12.4
Q5ZHW5	proteasome subunit α type; <i>Gallus gallus</i>	Pr	MP	CA	24.7	1	11.8
Q5ZKP5	putative uncharacterized protein; <i>Gallus gallus</i>	Cy	MP	CA	10.1	4	11.2
Q5ZL78	tumor necrosis factor α -induced protein 8; <i>Gallus gallus</i>	Cy	CDi	PB	10.6	1	10.6
Q5ZML5	protein LSM12 homologue; <i>Gallus gallus</i>			PB	11.3	2	10.3
A6ZJ09	NADH-ubiquinone oxidoreductase chain 5; <i>Anas platyrhynchos</i>	Mb	MP	CA		3	9.9
Q90WR6	sulfotransferase 1C; <i>Gallus gallus</i>	Cy	MP	CA	9.1	1	9.8
Q5ZJ49	putative uncharacterized protein; <i>Gallus gallus</i>	Cy	MP	CA	6.7	1	9.6
Q5ZIR0	putative uncharacterized protein; <i>Gallus gallus</i>	Mb			24.3	1	9.3
B5AG23	complement component 3d; <i>Anas platyrhynchos</i>	Mb		E		1	9.1
Q90ZK7	putative FK506-binding protein; <i>Gallus gallus</i>	Cy	MP	CA	9.3	1	8.8
P51890	lumican; <i>Gallus gallus</i>	EC		CA	7.9	2	8.7
Q5ZLY3	putative uncharacterized protein; <i>Gallus gallus</i>	Cy		PB	9.4	3	8.5
Q07718	ES/130 (fragment); <i>Gallus gallus</i>	Mb	T	Str	9.1	3	8.3
Q5ZL29	putative uncharacterized protein; <i>Gallus gallus</i>	Cy	MP	CA	7.8	2	8.1
Q5ZLV0	putative uncharacterized protein; <i>Gallus gallus</i>	Mb	T	PB	8.5	1	8.1
Q5ZJY1	putative uncharacterized protein; <i>Gallus gallus</i>		MP	CA	4.8	1	8.0
P05122	creatine kinase B-type; <i>Gallus gallus</i>	Cy		CA	7.1	1	7.9
Q5ZKH1	putative uncharacterized protein; <i>Gallus gallus</i>	Mb	CO	Str	6.9	1	7.7
A6ZJ08	NADH-ubiquinone oxidoreductase chain 4; <i>Anas platyrhynchos</i>	Mb	MP	CA		2	6.5
Q5ZMD2	ankyrin repeat and MYND domain-containing protein 2; <i>Gallus gallus</i>		MP	CA	5.2	2	6.5
Q5ZII4	putative uncharacterized protein; <i>Gallus gallus</i>		MP	CA	7.6	1	6.1
Q6EE60	ribosomal protein L18 (fragment); <i>Gallus gallus</i>	Ri	MP	Str	7.8	1	6.0
A6ZJ01	cytochrome <i>c</i> oxidase subunit 1; <i>Anas platyrhynchos</i>	Mb	MP	CA		2	5.8
Q90952	serum paraoxonase/arylesterase 2; <i>Gallus gallus</i>	Mb	MP	CA	2.5	1	5.6
Q5ZLW1	putative uncharacterized protein; <i>Gallus gallus</i>	Cy	MP	CA	5.2	2	5.6
P08642	GTPase HRas; <i>Gallus gallus</i>	Mb	CDi	CA	13.2	1	5.3
Q34160	cytochrome <i>b</i> ; <i>Cairina moschata</i>	Mb	MP	CA		2	5.3
Q98UJ7	branched-chain α -keto acid dehydrogenase E1- β subunit; <i>Gallus gallus</i>	Cy	MP	CA	4.3	1	5.1
Q5ZKP8	lysyl-tRNA synthetase; <i>Gallus gallus</i>	Cy	MP	CA	4.2	1	5.1

Table 4. Continued

sequence ref	protein name; taxonomy	CC	BP	MF	sequence coverage	peptide count	PAI
Q5ZK09	uncharacterized protein Cllorf73 homologue; <i>Gallus gallus</i>	Cy			6.6	1	5.1
Q5ZJL9	SAM domain and HD domain-containing protein 1; <i>Gallus gallus</i>	Nu	DR	CA	4.1	2	4.9
Q5ZLF6	putative uncharacterized protein; <i>Gallus gallus</i>	Mb	T		4.6	1	4.6
Q802A0	histidine ammonia-lyase; <i>Gallus gallus</i>	Cy	MP	CA	6.2	2	4.5
Q6U7I1	isoform 1 of ubiquitin carboxyl-terminal hydrolase 7; <i>Gallus gallus</i>	Nu	MP	CA	5.4	3	4.5
Q5ZM11	arginyl-tRNA synthetase, cytoplasmic; <i>Gallus gallus</i>	Cy	MP	CA	3.8	1	4.5
Q5ZMN7	putative uncharacterized protein; <i>Gallus gallus</i>	Cy	MP	CA	3.5	2	4.4
Q5F3X5	putative uncharacterized protein; <i>Gallus gallus</i>			PB	6	1	4.1
Q5ZK86	putative uncharacterized protein; <i>Gallus gallus</i>	Cy	MP	CA	4.8	1	4.0
Q5ZJP4	putative uncharacterized protein; <i>Gallus gallus</i>		MP	CA	6.7	1	3.7
Q9PWC6	ubiquitin carboxyl-terminal hydrolase; <i>Gallus gallus</i>				3.1	3	3.6
Q5ZL34	cleavage and polyadenylation specificity factor subunit 6; <i>Gallus gallus</i>	Nu	MP	NB	6.9	1	3.6
Q5ZLI9	putative uncharacterized protein; <i>Gallus gallus</i>	Cy	MP	CA	3	1	3.0
Q8AWB7	SMC1 protein cohesin subunit; <i>Gallus gallus</i>	Mb	CO	CA	2.3	1	2.4
P47990	xanthine dehydrogenase/oxidase; <i>Gallus gallus</i>	Cy	CDi	CA	3.3	1	2.2
Q5ZME3	putative uncharacterized protein; <i>Gallus gallus</i>		MP	CA	1.1	1	0.9
Q5ZIC1	putative uncharacterized protein; <i>Gallus gallus</i>	Cv	CC	CA	1.5	1	0.8

^aThe main cellular component (CC), biological process (BP) and molecular function (MF) are presented for each protein. The peptide count corresponds to peptide with a FDR < 1.3%. The protein abundance index (PAI) is calculated as indicated in Material and Methods. Abbreviations: (cellular component) Cy, cytoplasm; Csk, cytoskeleton; EC, extracellular; Go, Golgi apparatus; Mb, membrane; Nu, nucleus; Pr, proteasome; Ri, ribosome; Sp, spliceosome; (biological process) CC, cell communication; CDi, cell differentiation; CM, cell motility; CO, cell organization; COa, coagulation; DR, defense response; MP, metabolic process; RBP, regulation of biological process; RS, response to stimulus; T, transport; (molecular function) CA, catalytic activity; E, enzyme regulator activity; MB, metal ion binding; NB, nucleotide binding; PB, protein binding; Sig, signal transducer activity; Str, structural molecule activity; T, transporter activity; TA, translation regulator activity.

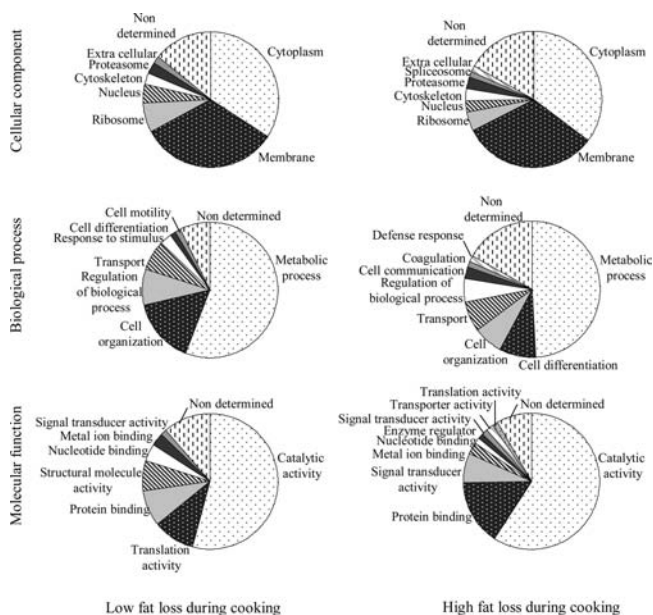


Figure 4. Distribution of main cellular component, biological process, and molecular function in both groups of fat loss, for specific proteins in low ($n = 70$) and high ($n = 71$) fat loss group, in the NS protein fraction.

dynamic synthesis of constituents and particularly proteins. To validate this result, we chose to study more specifically the mitochondrial carrier homologue protein (MIMP). We performed Western blot analysis on a second set of samples to make a validation on a biological replicate. We analyzed the expression of MIMP in each fat loss group (Figure 5). The results showed a higher expression in the low fat loss group, which is

Table 5. Analysis with the GO Database of the 13 Groups of Proteins from NS Fraction Over-represented in the Low Fat Loss Group

Cellular Component
ribosome $p = 5.3 \times 10^{-5}$
ribosomal subunit $p = 4.8 \times 10^{-4}$
eukaryotic translation initiation factor 3 complex $p = 4.8 \times 10^{-4}$
ribonucleoprotein $p = 5.2 \times 10^{-4}$
Biological Process
translation $p = 2.3 \times 10^{-5}$
formation of translation initiation complex $p = 5.3 \times 10^{-5}$
Molecular Function
structural constituent of ribosome $p = 5.2 \times 10^{-5}$
translation factor activity, nucleic acid binding $p = 1.0 \times 10^{-3}$
rRNA binding $p = 3.0 \times 10^{-3}$

consistent with results obtained by shot-gun approach. The MIMP could thus be a good marker of the fat loss during cooking early post-mortem.

Comparison of the localization of the proteins (474 clusters) detected in both samples did not reveal any differences. Approximately half of the proteins are involved in metabolic processes (Figure 4), regardless of the fat loss during cooking, which is consistent with the result of molecular function, which showed that more than half of these proteins have catalytic activity (Figure 4). These results confirm the relevance of using the shotgun method for the analysis of the NS protein fraction because a larger spectrum of cellular components is pointed out by this method compared to 2D electrophoresis.

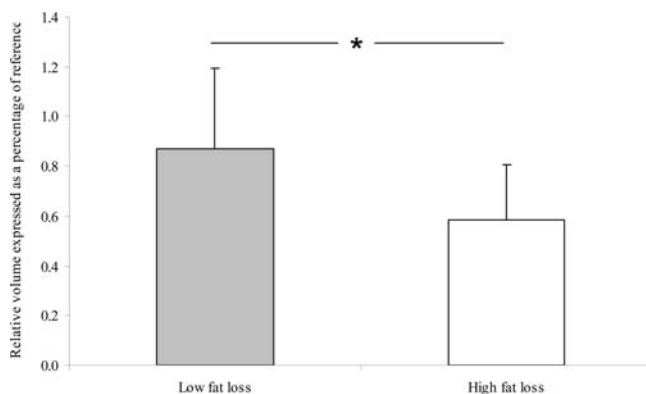


Figure 5. Relative amounts of MIMP protein obtained by using Western blots from NS protein fraction at 20 min post-mortem. For each fat loss group ($n = 13$ and 11 for low and high fat loss, respectively), results are reported as the mean \pm standard deviation.

The results obtained from both protein fractions were consistent and demonstrated the complementarity of both methods in the study of liver physiology. Despite the low number of identified spots, the proteomic analysis of the protein fraction soluble at low ionic strength early post-mortem allowed us to better understand the phenomenon of fat loss during cooking. Overall, in the livers that will have a low fat loss during cooking, the anabolism pathways are more intense, whereas in the livers that will have a high fat loss during cooking, the overexpressed proteins are mainly involved in oxidoreduction processes, probably because they reached a more advanced biological stage of steatosis. We can hypothesize that differences in the ability to accumulate lipids in the liver may lead to various states of steatosis development after a standard period of overfeeding, thus explaining part of the variability in the technological quality observed under industrial conditions. These results are in agreement with practical observations showing that a reduced duration of overfeeding improves the technological yield of duck fatty livers by reducing the fat loss during cooking.

AUTHOR INFORMATION

Corresponding Author

*Phone: +33 5 34 32 39 06. Fax: +33 5 34 32 39 01. E-mail: molette@ensat.fr.

Funding Sources

The financial supports of INRA, CIFO, and Région Midi-Pyrénées enabled the implementation of this project.

ACKNOWLEDGMENT

Ducks were slaughtered and processed under the facilities of the Lycée Agricole de Périgueux (EPLEFPA, 24, France). We are indebted to François Héroult (EPLEFPA) for technical supervision of the slaughter process and to Hélène Manse, Madonna Chin, Romain Dinis, Corinne Pautot, and Stéphane Seidlinger for technical assistance. We thank Alain Vignal (UMR INRA INPT, LGC) for kindly providing the duck EST database for protein identifications and Christine Rousseau (INP ENSAT) for setting up the database.

REFERENCES

(1) Journal Officiel de la République Française, 1993, Décret n° 93-9-99 du 09-08-93 du JO du 14-08-93, relatif aux préparations à base de foie gras.

(2) Rousselot-Pailley, D.; Guy, G.; Gourichon, D.; Sellier, N.; Blum, J. C. Influence des conditions d'abattage et de réfrigération sur la qualité des foies gras d'oie. *INRA, Prod. Anim.* **1992**, *5*, 167–172.

(3) Latil, G.; Auvergne, A.; Babilé, R. Consommation du canard mulard en gavage. Relation avec les performances zootechniques et la qualité du foie gras. *2ème Journées de la Recherche sur les Palmipèdes à Foie Gras, Bordeaux, France* **1996**, 93–97.

(4) Baudonnet-Lenfant, C.; Auvergne, A.; Babilé, R. Influence de la durée de jeûne avant l'abattage et du poids à la mise en gavage des canards de Barbarie sur la composition chimique hépatique. *Ann. Zoot.* **1991**, *40*, 161–170.

(5) Bouillier-Oudot, M.; Leprettre, S.; Dubois, J. P.; Babilé, R. Itinéraires *post mortem* et caractéristiques technologiques et organoleptiques des foies gras d'oies. *Sème Journées de la Recherche sur les Palmipèdes à Foie Gras, Pau, France* **2002**, 172–175.

(6) Blum, J. C.; Salichon, M. R.; Guy, G.; Rousselot-Pailley, D. Comparative development, chemical composition and quality of ducks and goose 'foie gras' obtained by cramming. *XIX World's Poultry Congress*; WPSA: Amsterdam, The Netherlands, 1992; pp 240244

(7) Baudonnet, C. *Facteurs de variation de la composition biochimique et de la qualité technologique des foies gras de canards*. Thèse de Doctorat, INP, Toulouse, France, 1993.

(8) Molee, W.; Bouillier-Oudot, M.; Auvergne, A.; Babilé, R. Changes in lipid composition of hepatocyte plasma membrane induced by overfeeding in duck. *Comp. Biochem. Physiol. Part B* **2005**, *141*, 437–444.

(9) Folch, J.; Lees, M.; Sloane Stanley, G. H. A simple method for the isolation and purification of total lipids from animal tissue. *J. Biol. Chem.* **1957**, *226*, 497–509.

(10) Bergmeyer, H. U. In *Methods of Enzymatic Analysis*; Bourne, G. H., Ed.; Academic Press: New York, 1974; pp 1127, 1196, 1238, 1464.

(11) Oliver, C. N.; Alin, B. W.; Moerman, E. J.; Goldstein, S.; Stadtman, E. R. Age related changes in oxidized proteins. *J. Biol. Chem.* **1987**, *262*, 5488–5491.

(12) Mercier, Y.; Gatellier, Ph.; Viau, M.; Réminon, H.; Renner, M. Effect of dietary fat and vitamin E on lipid and protein oxidation in turkey meat during storage. *Meat Sci.* **1998**, *48*, 301–317.

(13) Lynch, S. M.; Frey, B. Mechanisms of copper- and iron-dependent oxidative modification of human low density lipoprotein. *J. Lipid Res.* **1993**, *34*, 1745–1751.

(14) Sayd, T.; Morzel, M.; Chambon, C.; Franck, M.; Figwer, P.; Larzul, C.; Le Roy, P.; Monin, G.; Cherel, P.; Laville, E. Proteome analysis of the sarcoplasmic fraction of pig semimembranous muscle: Implications on meat color development. *J. Agric. Food Chem.* **2006**, *54* (7), 2732–2737.

(15) Morzel, M.; Chambon, C.; Lefèvre, F.; Paboef, G.; Laville, E. Modification of trout (*Oncorhynchus mykiss*) muscle proteins by pre-slaughter activity. *J. Agric. Food Chem.* **2006**, *54*, 2997–3001.

(16) Meunier, B.; Bouley, J.; Picc, I.; Bernard, C.; Picard, B.; Hocquette, J. F. Data analysis methods for detection of differential protein expression in two-dimensional gel electrophoresis. *Anal. Biochem.* **2005**, *340*, 226–230.

(17) Laemmli, U. K. Cleavage of structural proteins during the assembly of the head of bacteriophage T4. *Nature* **1970**, *227*, 680–685.

(18) Borderies, G.; Jamet, E.; Lafitte, C.; Rossignol, M.; Jauneau, A.; Boudart, G.; Monsarrat, B.; Esquerré-Tugayé, M. T.; Boudet, A.; Pont-Lezica, R. Proteomics of loosely bound cell wall proteins of *Arabidopsis thaliana* cell suspension cultures: a critical analysis. *Electrophoresis* **2003**, *24*, 3421–3432.

(19) Bouyssié, D.; Gonzales de Peredo, A.; Mouton, E.; Albigot, R.; Roussel, L.; Ortega, N.; Cayrol, C.; Burlet-Schiltz, O.; Girard, J. P.; Monsarrat, B. Mascot file parsing and quantification (MFPaQ), a new software to parse, validate and quantify proteomics data generated by ICAT and SILAC mass spectrometric analyses: application to the proteomics study of membrane proteins from primary human endothelial cells. *Mol. Cell Proteomics* **2007**, *6* (9), 1621–1637.

(20) Liu, H.; Sadygov, R. G.; Yates, J. A model for random sampling and estimation of relative protein abundance in shotgun proteomics. *Anal. Chem.* **2004**, *76* (14), 4193–4201.

(21) Zhu, M.; Smith, J. W.; Huang, C. M. Mass spectrometry-based label-free quantitative proteomics. *J. Biomed. Biotechnol.* **2010**, doi: 10.1155/2010/840518.

(22) Towbin, H.; Staehelin, T.; Gordon, J. Electrophoresis transfer of proteins from polyacrylamide gels to nitrocellulose sheets: procedure and some applications. *Proc. Natl. Acad. Sci. U.S.A.* **1979**, *76*, 4350–4354.

(23) Zhu, L. H.; Meng, H.; Duan, X. J.; Xu, G. Q.; Zhang, J.; Qong, D. Q. Gene expression profile in the liver tissue of geese after over-feeding. *Poult. Sci.* **2011**, *90*, 107–117.

(24) Bax, M. L.; Chambon, C.; Marty-Gasset, N.; Rémignon, H.; Fernandez, X.; Molette, C. Proteomic profile evolution during steatosis development in duck. *Poult. Sci.* **2011** (DOI: 10.3382/ps.2011-01663).

(25) Greco, D.; Kotronen, A.; Westerbacka, J.; Puig, O.; Arkkila, P.; Kiviluoto, T.; Laitinen, S.; Fisher, R. M.; Hamsten, A.; Auvinen, P.; Yki-Järvinen, H. Gene expression in human NAFLD. *Am. J. Physiol. Gastrointest. Liver Physiol.* **2008**, *294*, 1281–1287.

(26) Jo, C.; Ahn, D. U. Fluorometric analysis of 2-thiobarbituric acid reactive substances in turkey. *Poult. Sci.* **1999**, *77*, 475–480.

(27) Iff, J.; Wang, W.; Sajic, T.; Oudry, N.; Gueneau, E.; Hopfgartner, G.; Varesio, E.; Szanto, I. Differential proteomic analysis of STAT6 knockout mice reveals new regulatory function in liver lipid homeostasis. *J. Proteome Res.* **2009**, *8*, 4511–4524.

(28) Sreekumar, R.; Rosado, B.; Rasmussen, D.; Charlton, M. Hepatic gene expression in histologically progressive nonalcoholic steatohepatitis. *Hepatology* **2003**, *38* (1), 244–251.

(29) Yamaguchi, M. Role of regucalcin in calcium signaling. *Life Sci.* **2000**, *66* (19), 1769–1780.

(30) Yamaguchi, M.; Kanayama, Y. Enhanced expression of calcium binding protein regucalcin mRNA in regenerating rat liver. *J. Cell Biochem.* **1995**, *57* (2), 185–190.

(31) Roberts, L. R.; Adjei, P. N.; Gores, G. J. Cathepsins as effector proteases in hepatocytes apoptosis. *Cell Biochem. Biophys.* **1999**, *30*, 71–88.

(32) Kirpich, I. A.; Gobejishvili, L. N.; Bon Homme, M.; Waigel, S.; Cave, M.; Arteel, G.; Barve, S. S.; McClain, C. J.; Deaciuc, I. V. Integrated hepatic transcriptome and proteome analysis of mice with high-fat diet-induced nonalcoholic fatty liver disease. *J. Nutr. Biochem.* **2010**, *22* (1), 38–45.

(33) Federico, A.; Tuccillo, C.; Terracciano, F.; D'Alessio, C.; Galdiero, M.; Finamore, E.; D'Isanto, M.; Peluso, L.; Del Vecchio Blanco, C.; Loguercio, C. HSP 27 expression in patients with chronic liver damage. *Immunobiology* **2005**, *209*, 729–735.

(34) Mölleken, C.; Sitek, B.; Henkel, C.; Poschmann, G.; Sipos, B.; Wiese, S.; Warscheid, B.; Broelsch, C.; Reiser, M.; Friedman, S. L.; Tornøe, I.; Schlosser, A.; Klöppel, G.; Schmiegel, W.; Meyer, H. E.; Holmskov, U.; Stühler, K. Detection of novel biomarkers of liver cirrhosis by proteomic analysis. *Hepatology* **2009**, *49* (4), 1257–1266.

(35) Atzori, L.; Poli, G.; Perra, A. Hepatic stellate cell: a star cell in the liver. *Int. J. Biochem. Cell Biol.* **2009**, *41*, 1639–1642.

(36) Bénard, G.; Labie, Ch. Evolution histologique du foie des palmipèdes au cours du gavage. *3ème Journées de la Recherche sur les Palmipèdes à Foie Gras, Bordeaux, France* **1998**, 31–35.

(37) Gabarrou, J. F.; Salichon, M. R.; Guy, G.; Blum, J. C. Hybrid ducks overfed with boiled corn develop an acute hepatic steatosis with decreased choline and polyunsaturated fatty acid level in phospholipids. *Reprod. Nutr. Dev.* **1996**, *36*, 473–484.